


Dynamical susceptibilities near ideal glass transitions

Corentin C. L. Laudicina,¹ Chengjie Luo¹, Kunimasa Miyazaki², and Liesbeth M. C. Janssen^{1,*}

¹*Soft Matter & Biological Physics, Department of Applied Physics, Eindhoven University of Technology,
P.O. Box 513, 5600MB Eindhoven, The Netherlands*

²*Department of Physics, Nagoya University, Nagoya 464-8602, Japan*

 (Received 12 August 2022; revised 11 November 2022; accepted 28 November 2022; published 28 December 2022)

Building on the recently derived inhomogeneous mode-coupling theory, we extend the generalized mode-coupling theory of supercooled liquids to inhomogeneous environments. This provides a first-principles-based, systematic, and rigorous way of deriving high-point dynamical susceptibilities from variations of the many-body dynamic structure factors with respect to their conjugate field. This framework allows for a fully microscopic possibility to probe for collective relaxation mechanisms in supercooled liquids near the mode-coupling glass transition. The behavior of these dynamical susceptibilities is then studied in the context of simplified self-consistent relaxation models.

DOI: [10.1103/PhysRevE.106.064136](https://doi.org/10.1103/PhysRevE.106.064136)

I. INTRODUCTION

The past 40 years have been very fruitful in progress regarding the theoretical nature of the glass transition. Among the most prominent microscopic theories of the glass transition we find the mode-coupling-theory [1–3] and the replica theory for the structural glass transition [4,5]. Their respective success relies on their ability to predict critical temperatures pertaining to an ergodicity breaking-event, which has been speculated in structural glasses in the past. However, the emergence of dynamical heterogeneities at the onset of glass formation [6–19] remains one of the most poorly understood facet of glass forming liquids to date. These dynamic structures arise as correlated clusters of transiently mobile particles coexisting with regions of immobile particles. The existence of these correlated clusters is in line with the earliest phenomenological approaches to the glass transition of Adam-Gibbs [20], where the concept of “cooperatively rearranging regions” was first introduced. Dynamical heterogeneity appears to be a universal feature among glass formers [15] and was also observed in athermal systems near the jamming point [21,22] and in dense active systems [23–26]. More recently, studies focused on the morphology of these correlated clusters, determining preferential structural ordering in fast and slow moving clusters [27], as well as their fractal dimension and compactedness [28–30]. Yet the understanding of dynamical heterogeneity, its origin, and consequences with regards to the observed experimental dynamical arrest stand as important missing pieces in the physics of the glass transition.

The established standard measure of dynamical heterogeneity takes the form of a four-point dynamical susceptibility denoted $\chi_4(t)$ [6,11,12,14–19]. In analogy with critical phenomena, $\chi_4(t)$ is generally defined as the variance of some mobility field, say $\mu(\mathbf{r}, t)$, which quantifies the mobility of a

particle initially located at position \mathbf{r} and time t . Dynamical heterogeneity is captured by the covariance of such a mobility field in both space and time. Mathematically we may write $\text{cov}[\mu(\mathbf{r}, t)\mu(\mathbf{r}', t')] \propto G_4(\mathbf{r}, t; \mathbf{r}', t') = G_4(\mathbf{r} - \mathbf{r}', t - t')$ using spatial and time translation invariance. The four-point susceptibility is then given by the spatial integration of $G_4(\mathbf{r}, t - t')$

$$\begin{aligned} \chi_4(t - t') &= \int d\mathbf{r} G_4(\mathbf{r}, t - t') \\ &\sim \int d\mathbf{r} B(\mathbf{r}, t - t') e^{-|\mathbf{r}|/\xi_4(t-t')}, \end{aligned} \quad (1)$$

where $\xi_4(t)$ is the dominant dynamical lengthscale associated with the heterogeneities and $B(\mathbf{r}, t - t')$ some scaling function [31]. The name “four-point” stems from the fact that the mobility field is generally a two-point function already [15]. Numerous studies (both experimental and numerical) [8,9,15,32,33] demonstrate that such four-point susceptibilities grow in a peak-like manner as the experimental glass transition is approached. The peak is generally identified to occur for times of order $t \sim \mathcal{O}(\tau_\alpha)$ with τ_α representing the structural relaxation timescale of the system. The fact that dynamical heterogeneity manifests itself in both space and time implies that on timescales $t \gg \tau_\alpha$ the four-point susceptibility decays to zero. However, the persistence of dynamical clusters beyond τ_α have also recently been reported [17].

In the mildly supercooled regime, a wide array of glass-forming materials display a power law growth $\chi_4(\tau_\alpha) \sim \tau_\alpha^{1/\gamma}$ with a smooth crossover to a logarithmic growth $\chi_4(\tau_\alpha) \sim \ln(\tau_\alpha)^{1/\psi}$ close to the experimental glass transition, see [34] and references therein. Unfortunately, obtaining an accurate measure of $\chi_4(t)$ in the supercooled regime is a complicated task both computationally and experimentally. Indeed, measuring four-point susceptibilities requires long temporal (several decades) and extensive spatial resolutions (subparticle radii resolution over large lengthscales) since one is

*l.m.c.janssen@tue.nl

probing for correlations in spontaneous fluctuations of the mobility field. Furthermore, some have reported that this four-point susceptibility is highly anisotropic [35], while most studies considered angularly averaged susceptibilities. The four-point susceptibilities were also found to bear nontrivial dependences on the choice of both dynamics and statistical ensemble in which simulations are performed [36,37]. It would be of interest to have a more consistent way to measure dynamical heterogeneity spanning all approaches to the glass problem: theories, simulations, and experiments.

II. THEORY

Equation (1) defines the dynamic lengthscale $\xi_4(t)$ over which the dynamics are strongly correlated in time. While the existence of a strictly diverging dynamic lengthscale at the structural glass transition remains debated in the field, it is clear that there exists at least an emerging and growing one from the combination of numerical and experimental results available [38–42]. This provides a basis for a viable critical phenomena-like description of glass formation [43] and is the motivation for the present work.

Within the Landau formalism of second-order phase transitions, a susceptibility is defined as the functional variation of the order parameter with respect to its conjugate field. A common order parameter to detect the glassy phase is the collective intermediate scattering function $F_2(\mathbf{k}, t) \propto \langle \hat{\rho}_{\mathbf{k}}^*(0) \hat{\rho}_{\mathbf{k}}(t) \rangle_0$ where $\hat{\rho}_{\mathbf{k}}(t)$ is a collective density fluctuation mode at wave vector \mathbf{k} and time t :

$$\hat{\rho}_{\mathbf{k}}(t) = \sum_{j=1}^N e^{i\mathbf{k}\cdot\mathbf{r}_j(t)} - \left\langle \sum_{j=1}^N e^{i\mathbf{k}\cdot\mathbf{r}_j(t)} \right\rangle_0. \quad (2)$$

The statistical averaging $\langle \dots \rangle_0$ is performed with respect to the Hamiltonian of a homogeneous (i.e., field-free and thus translationally invariant) system. By interpreting the equation of motion for this order parameter as a dynamical Landau theory, the associated susceptibility is obtained by considering variations of this order parameter with respect to its conjugate field that we denote $U(\mathbf{q}_0)$. For the purpose of the theoretical development, the simplest consideration is an arbitrary field that couples to the local density. In practice, one would need an external disturbance which locally modulates the density field such as a spatially oscillating electric field. This dynamic susceptibility, denoted as $\vartheta_3(t)$, reads

$$\lim_{U \rightarrow 0} \frac{\delta F_2(\mathbf{k}; \mathbf{k}', t)}{\delta U(\mathbf{q}_0)} = \vartheta_3(\mathbf{k}; \mathbf{k}', \mathbf{q}_0, t), \quad (3)$$

where $F_2(\mathbf{k}; \mathbf{k}', t) \propto \langle \hat{\rho}_{\mathbf{k}}^* \hat{\rho}_{\mathbf{k}'}(t) \rangle$ is written with two explicit wave-number modes because the presence of the pinning field U breaks translational invariance. This type of three-point susceptibility was first proposed as an alternative to $\chi_4(t)$ [36,37,44–46]. The four-point and three point susceptibilities are intimately linked quantities. If the conjugate field is assumed to be the density field, a simple combination of the Cauchy-Schwartz inequality and the fluctuation dissipation theorem leads to the conclusion that $\chi_4(t) \geq \rho_0 \kappa_T \beta^{-1} [\vartheta_3(t)]^2$ [36,47], where ρ_0 is the bulk-fluid density, κ_T the isothermal compressibility, and β the inverse temperature of the system

under consideration. Similar expressions can be derived in the case of different conjugate fields.

The three-point susceptibility has the advantage of being much easier to determine than the four-point one, as obtaining good-enough statistics to take the derivative of the intermediate scattering function is easier than obtaining a statistically relevant four-point correlation function. Following its introduction, several groups were able to extract this three-point susceptibility from high-precision dielectric spectroscopy experiments in canonical glass forming materials [47–52], as well as in molecular dynamics simulations [53,54]. In this light, the mode-coupling theory (MCT) [2,3] (a more recent exposition can be found in [55,56]) of the glass transition was then extended to the presence of external fields [46] and, interpreting it as a Landau theory [43], an equation of motion for the three-point susceptibility Eq. (3) was derived.

Here we consider multipoint susceptibilities that arise when going beyond the standard MCT. For this we use the framework of so-called generalized mode-coupling theory (GMCT) [57,58], which is an extended theory that has been shown to quantitatively improve on some of the weaknesses of MCT [57–64]. These weaknesses can, in part, be traced back to an unjustified Wick factorization made to obtain a self-consistent equation of motion for $F_2(\mathbf{k}, t)$. The GMCT effectively delays this uncontrolled approximation by including physical higher-order density correlations in the picture. Such higher-order density correlation functions are defined as straight generalizations to $F_2(\mathbf{k}, t)$: $F_{2n}(\mathbf{k}_1, \dots, \mathbf{k}_n, t) \propto \langle \hat{\rho}_{\mathbf{k}_1}^* \dots \hat{\rho}_{\mathbf{k}_n}^* \hat{\rho}_{\mathbf{k}_1}(t) \dots \hat{\rho}_{\mathbf{k}_n}(t) \rangle$. This property of the GMCT which enables the treatment of an arbitrary number of multipoint correlation functions F_{2n} , provides direct access to the higher-order dynamical susceptibilities defined as straight generalizations to Eq. (3)

$$\begin{aligned} \vartheta_{2n+1}(\mathbf{k}_1, \dots, \mathbf{k}_n; \mathbf{k}_1, \dots, \mathbf{k}_n, \mathbf{q}_0, t) \\ \equiv \lim_{U \rightarrow 0} \frac{\delta F_{2n}(\mathbf{k}_1, \dots, \mathbf{k}_n; \mathbf{k}_1, \dots, \mathbf{k}_n, t)}{\delta U(\mathbf{q}_0)}. \end{aligned} \quad (4)$$

These new collective responses are expected to shed light on heterogeneous dynamics near the GMCT transition line. In particular, these susceptibilities provide a way to systematically study responses of many-body relaxation processes to controlled perturbations in both space and time, something which has been missing from the conventional treatments of dynamical heterogeneity.

The paper is organized as follows. In the next part, the GMCT is extended to inhomogeneous environments by appropriately considering a spatially varying external field $U(\mathbf{r})$ chosen to couple to the density modes. This framework is referred to as inhomogeneous generalized mode-coupling theory (IGMCT). By treating the equations of motion in reciprocal space for the $2n$ -point correlators as a Landau theory [43], their functional variations with respect to the external field $U(\mathbf{q}_0)$ then results in an equation of motion for the odd-point susceptibilities $\vartheta_{2n+1}(t)$ of any order which can, in turn, be solved self-consistently once a closure relation for IGMCT has been determined. Then, the developed equations of motion are mapped onto a simplified self-consistent relaxation model inspired by earlier studies of schematic mode-coupling

theories. A detailed numerical study of the simplified models is also provided.

A. Inhomogeneous generalized mode-coupling theory

Consider a classical Newtonian interacting fluid composed of N_p particles in the presence of an arbitrary spatially varying external field $U(\mathbf{r})$ that modulates the density field $\rho(\mathbf{r})$. Let $\langle \dots \rangle$ denote statistical averaging with respect to the inhomogeneous Hamiltonian. Working in Fourier (reciprocal) space, the first set of dynamical variables of interest for GMCT are time-dependent density fluctuation multiplets, denoted as $A_{\mathbf{k}_1, \dots, \mathbf{k}_n}^{(n)}(t) \equiv \prod_{j=1}^n \hat{\rho}_{\mathbf{k}_j}(t)$ where $n = 1, 2, \dots$, and $\hat{\rho}_{\mathbf{k}}(t) = \sum_{l=1}^{N_p} e^{i\mathbf{k} \cdot \mathbf{r}_l(t)} - \langle \rho_{\mathbf{k}} \rangle$ is a density fluctuation. The second set of dynamical variables of interest are the projected density currents, proportional to the time derivative of the fluctuation multiplet: $\dot{A}_{\mathbf{k}_1, \dots, \mathbf{k}_n}^{(n)}(t)$. By construction, at equal times (taken to be zero without loss of generality), the correlation of density-density multiplets is proportional to the $2n$ -body static structure factor $S_{2n}: \langle A_{\mathbf{k}_1, \dots, \mathbf{k}_n}^{(n)}(0) A_{\mathbf{k}'_1, \dots, \mathbf{k}'_n}^{(n)}(0) \rangle = N_p S_{2n}(\mathbf{k}_1, \dots, \mathbf{k}_n; \mathbf{k}'_1, \dots, \mathbf{k}'_n) \delta(\sum_{j=1}^n (\mathbf{k}_j - \mathbf{k}'_j) - \mathbf{q}_0)$, while the proper autocorrelation of density-density multiplets is proportional to the $2n$ -body dynamic structure factor denoted $F_{2n}: \langle A_{\mathbf{k}_1, \dots, \mathbf{k}_n}^{(n)}(0) A_{\mathbf{k}'_1, \dots, \mathbf{k}'_n}^{(n)}(t) \rangle = N_p F_{2n}(\mathbf{k}_1, \dots, \mathbf{k}_n; \mathbf{k}'_1, \dots, \mathbf{k}'_n, t) \delta(\sum_{j=1}^n (\mathbf{k}_j - \mathbf{k}'_j) - \mathbf{q}_0)$. Here \mathbf{q}_0 is the wave vector corresponding to the localized perturbation induced by the external field $U(\mathbf{q}_0)$, and the Dirac δ function is included to enforce total momentum conservation. For reasons of notational clarity, these momentum enforcing δ functions will be omitted in the results below. Furthermore, a condensed notation for function arguments is used: $\{\mathbf{k}_j\}_{l:m/p} \equiv (\mathbf{k}_l, \mathbf{k}_{l+1}, \dots, \mathbf{k}_{m-1}, \mathbf{k}_m)$ in which \mathbf{k}_p is omitted.

Using the standard Mori-Zwanzig projector formalism [65–68] [see Supplemental Material (SM) [69], which also includes additional references [70–73]], the following equation of motion for the $2n$ -body dynamic structure factors can be derived:

$$\begin{aligned} 0 = & \ddot{F}_{2n}(\{\mathbf{k}_j\}_{1:n}; \{\mathbf{k}_j\}_{n+1:2n}, t) + v_{2n} \dot{F}_{2n}(\{\mathbf{k}_j\}_{1:n}; \{\mathbf{k}_j\}_{n+1:2n}, t) \\ & + \sum_{i=1}^n \int d\mathbf{k} \Omega^2(\mathbf{k}; \mathbf{k}) F_{2n}(\mathbf{k}_i, \{\mathbf{k}_j\}_{1:n/i}; \{\mathbf{k}_j\}_{n+1:2n}, t) \\ & + \frac{1}{n!} \int_0^t d\tau \int d\{\mathbf{k}'_j\}_{1:n} \mathcal{M}_{2n}(\{\mathbf{k}_j\}_{1:n}; \{\mathbf{k}'_j\}_{1:n}, t - \tau) \\ & \times \dot{F}_{2n}(\{\mathbf{k}'_j\}_{1:n}; \{\mathbf{k}_j\}_{n+1:2n}, \tau), \end{aligned} \quad (5)$$

where the quantity $\Omega^2(\mathbf{k}; \mathbf{k}')$ is commonly referred to as a bare frequency (due to its physical dimension). The bare frequency term can explicitly be written as

$$\Omega^2(\mathbf{k}; \mathbf{k}') = \frac{k_B T}{m} \int d\mathbf{p} (\mathbf{k} \cdot \mathbf{p}) \phi(\mathbf{k} - \mathbf{p}) S^{-1}(\mathbf{p}; \mathbf{k}'), \quad (6)$$

where $\phi(\mathbf{k}) = N_p^{-1} \langle \hat{\rho}_{\mathbf{k}} \rangle$ is the average of a single density mode. Equation (6) above has a form very similar to that of homogeneous GMCT [58] and reduces to it upon taking the zero-field limit. Indeed, in both the homogeneous and inhomogeneous cases, the bare frequencies of higher-order

correlators are simply equal to a sum of two-body bare frequencies. Further, we note that the term $v_{2n} \dot{F}_{2n}$ emerges from the splitting of the memory kernel into a term containing the effects of the density fluctuations and v_{2n} , generally referred to as the “regular” contributions to the memory kernel, which are assumed to be δ correlated in time and to only matter for short-term dynamics. In principle, the regular contributions should also be wave-number dependent, but for all practical calculations they are generally set to unity. This decomposition is standard in mode-coupling approaches to liquid dynamics [2,3].

The integral kernel $\mathcal{M}_{2n}(t)$ is known as the $2n$ th memory function. At each level n of the hierarchy, the integral kernel admits contributions from a product of $(n+1)$ density modes, as detailed in the SM. To leading order then, it is possible to show that $\mathcal{M}_{2n}(t) \propto F_{2(n+1)}(t)$ [57,58]. This is precisely what is meant by a hierarchy of coupled integrodifferential equations that successively involves higher-order density correlation functions. Explicitly, the memory kernel reads

$$\begin{aligned} \mathcal{M}_{2n}(\{\mathbf{k}_j\}_{1:n}; \{\mathbf{k}'_j\}_{1:n}, t) &= \frac{1}{[(n+1)!]^2 n!} \int d\{\mathbf{k}'_j\}_{1:n} d\{\mathbf{q}_j\}_{1:n+1} d\{\mathbf{q}'_j\}_{1:n+1} \\ &\times \mathcal{V}_{2n}^\dagger(\{\mathbf{k}_j\}_{1:n}; \{\mathbf{q}_j\}_{1:n+1}) F_{2(n+1)}(\{\mathbf{q}_j\}_{1:n+1}; \{\mathbf{q}'_j\}_{1:n+1}, t) \\ &\times \mathcal{V}_{2n}(\{\mathbf{k}'_j\}_{1:n}; \{\mathbf{q}'_j\}_{1:n+1}) J_{2n}^{-1}(\{\mathbf{k}'_j\}_{1:n}; \{\mathbf{k}'_j\}_{1:n}), \end{aligned} \quad (7)$$

where the time-independent factors \mathcal{V}_{2n} are c-numbers commonly referred to as vertices. These factors represent the effective coupling strengths between different density modes, hence the name “mode-coupling.” The detailed form of the vertices is presented in the SM.

In the vertex terms as well as the bare frequency term calculations, a Gaussian factorization [58] of $2n$ -body static structure factors and the corresponding inverses is used: $S_{2n}^{(-1)}(\{\mathbf{k}_j\}_{1:n}; \{\mathbf{k}'_j\}_{1:n}) \approx S_2^{(-1)}(\mathbf{k}_1; \mathbf{k}'_1) \times \dots \times S_2^{(-1)}(\mathbf{k}_n; \mathbf{k}'_n) + (n-1)!$ permutations over $\{\mathbf{k}'_j\}_{1:n}$. The vertices also contain another type of n -body static density correlations which are expressed as $S_{2n+1}(\{\mathbf{k}_j\}_{1:n}; \{\mathbf{k}'_j\}_{1:n+1}) = N_p^{-1} \langle A_{\mathbf{k}_1, \dots, \mathbf{k}_n}^{(n)}(0) A_{\mathbf{k}'_1, \dots, \mathbf{k}'_{n+1}}^{(n+1)}(0) \rangle$. In the homogeneous GMCT [57,58], such correlation functions are factorized in an ad hoc fashion using a mixture of three-body convolution [74,75] and Gaussian factorization approximations [58]. They are not factorized here to keep the equations of motion as formally exact as possible in light of the linear response expansion that follows. The last term of Eq. (7), J_{2n}^{-1} , is the inverse equal time correlation of the density currents.

Expression (5) then forms a hierarchy of coupled equations of motion for many-body dynamic structure factors for a glass forming monatomic liquid in the presence of an external field. While the formal limit $n \rightarrow \infty$ can be considered, it is common to self-consistently close the hierarchy at finite order by approximating $\mathcal{M}_{N_c}(t)$ at some hierarchy height N_c using products of lower-order many-body dynamic structure factors. This is what is called a “mean-field closure” in the generalized mode-coupling literature [58,60,61]. By setting $n = 1$ and applying the mode-coupling approximation $F_4(\mathbf{k}_1, \mathbf{k}_2; \mathbf{k}'_1, \mathbf{k}'_2, t) \approx F_2(\mathbf{k}_1; \mathbf{k}'_1, t) F_2(\mathbf{k}_2; \mathbf{k}'_2, t) + (\mathbf{k}'_1 \leftrightarrow \mathbf{k}'_2)$, the inhomogeneous MCT originally derived in [46] is

appropriately recovered. For the detailed derivation of IGMCCT at arbitrary order, we refer the reader to the SM.

Interestingly, taking the zero field limit ($U(\mathbf{q}_0) \rightarrow 0$) of Eq. (5) gives direct access to so-called off-diagonal GMCT (oGMCT) [76], which is a first-principles improvement upon the original GMCT. Indeed, the homogeneous GMCT derived in [58] only contains symmetric, angularly averaged n -body dynamic structure factors of the form $F_{2n}^{(0)}(k_1, \dots, k_n; k_1, \dots, k_n, t)$, thus neglecting the many-body correlations that correspond to physical processes where inelastic scattering of excitations would take place. oGMCT is an attempt to remedy this approximation by including off-diagonal modes in the theoretical framework. This flavor of GMCT was first derived self-consistently for $F_2^{(0)}$ and $F_4^{(0)}$ in [76]. A detailed study of oGMCT would provide important insights on structural glass formers and even possibly remedy the remaining deficiencies of [58–60], but the numerical evaluation of the full oGMCT framework is currently computationally infeasible.

B. Dynamical susceptibilities

To obtain the equations of motion for the many-body response functions $\vartheta_{2n+1}(\mathbf{q}_0; t)$ we consider the variation of Eq. (5) with respect to the external field. We recall that the response of the many-body dynamic correlation function is defined as $\vartheta_{2n+1}(\mathbf{q}_0; t) \equiv \lim_{U \rightarrow 0} \delta / \delta U(\mathbf{q}_0) F_{2n}(t)$. The conjugate variable to the field U is assumed to be a density mode $\hat{\rho}_{\mathbf{q}_0}$ [46,54]. By considering the functional variation of Eq. (5) with respect to the external field, it is easy to see that we obtain a linear hierarchy of coupled equations for the dynamical susceptibilities $\vartheta_{2n+1}(\mathbf{k}_1, \dots, \mathbf{k}_n; \mathbf{k}'_1, \dots, \mathbf{k}'_n, \mathbf{q}_0, t)$, which inherits the structure of the GMCT hierarchy. Indeed, the $(2n+1)$ th response depends on the $[2(n+1)+1]$ th one since the variation of the memory kernel \mathcal{M}_{2n} will result in $\mathcal{M}_{2n}^{(\vartheta)}(t) \propto \vartheta_{2(n+1)+1}(t)$. The self-consistency of the equations of motion for the response functions is uniquely determined by the chosen self-consistent closure of the GMCT hierarchy Eq. (5). In full, the $(2n+1)$ th susceptibility reads

$$\begin{aligned} & \ddot{\vartheta}_{2n+1}(\{\mathbf{k}_j\}_{1:n}; \{\mathbf{k}_j\}_{n+1:2n}, \mathbf{q}_0, t) + \nu_{2n} \dot{\vartheta}_{2n+1}(\{\mathbf{k}_j\}_{1:n}; \{\mathbf{k}_j\}_{n+1:2n}, \mathbf{q}_0, t) + \sum_{i=1}^n \frac{|\mathbf{k}_i|^2}{S(k_i)} \vartheta_{2n+1}(\mathbf{k}_i, \{\mathbf{k}_j\}_{1:n/i}; \{\mathbf{k}_j\}_{n+1:2n}, \mathbf{q}_0, t) \\ & + \frac{1}{n!} \int_0^t d\tau \int d\{\mathbf{k}'_j\}_{1:n} \mathcal{M}_{2n}^{(\vartheta)}(\{\mathbf{k}_j\}_{1:n}; \{\mathbf{k}'_j\}_{1:n}, \mathbf{q}_0, t - \tau) \dot{F}_{2n}(\{\mathbf{k}'_j\}_{1:n}; \{\mathbf{k}_j\}_{n+1:2n}) \\ & + \frac{1}{n!} \int_0^t d\tau \int d\{\mathbf{k}'_j\}_{1:n} \mathcal{M}_{2n}(\{\mathbf{k}_j\}_{1:n}; \{\mathbf{k}'_j\}_{1:n}, t - \tau) \dot{\vartheta}_{2n+1}(\{\mathbf{k}'_j\}_{1:n}; \{\mathbf{k}_j\}_{n+1:2n}, \mathbf{q}_0, \tau) = \mathcal{T}_{2n}(\{\mathbf{k}_j\}_{1:n}; \{\mathbf{k}_j\}_{n+1:2n}, \mathbf{q}_0, t), \quad (8) \end{aligned}$$

where the general functional \mathcal{T}_{2n} on the right-hand side consists of all terms generated by the field variation, which do not contain any susceptibilities (see SM). The equation of motion for the dynamical susceptibility is subject to the momentum conservation constraint $\sum_{j=1}^n \mathbf{k}_j - \sum_{j=n+1}^{2n} \mathbf{k}_j - \mathbf{q}_0 = 0$.

The left-hand side of Eq. (8) has the form of a linear integrodifferential operator, and may be compactly rewritten as $\hat{\mathcal{D}}_{2n} * \vartheta_{2n+1} = \mathcal{T}_{2n}$ where the term containing $\mathcal{M}_{2n}^{(\vartheta)}$ has been temporarily absorbed in \mathcal{T}_{2n} . We expect that the inversion of this operator $\hat{\mathcal{D}}_{2n}$ can lead to divergent behavior at the critical point, as is the case for conventional critical phenomena. Work along this line was previously done for the closely related four-point susceptibility in a field theoretic setting [45] whose operator actually corresponds to $\hat{\mathcal{D}}_2$ in the present case [45,46]. Two of the terms contained in \mathcal{T}_{2n} are linked to the response of the vertices (see SM). In the IMCT case, it was shown that $\delta \mathcal{V}_2 / \delta U \sim 0$ [46,77]. Given that the form of the vertices \mathcal{V}_{2n} amounts to linear combinations of \mathcal{V}_2 in a homogeneous setting [58], this result may be generalized within a suitable set of ad hoc factorization ansätze, such that the variation of vertices of any order is null: $\delta \mathcal{V}_{2n} / \delta U \sim 0$. This implies that the very same “mode-coupling” mechanisms are responsible for both the behavior of the many-body correlators and their associated susceptibilities. A detailed analysis of the operator $\hat{\mathcal{D}}_{2n}$ and particularly its inversion is, however, beyond the scope of this work.

The microscopic three-point susceptibility with truncation at hierarchy height $N_c = 1$ was numerically studied in the

past [78,79]. It was found that the dynamical lengthscale associated with $\vartheta_3(t)$ diverges as the ideal MCT transition is approached, confirming initial results [46] regarding the scaling behavior of the IMCT equations. In addition, similar three-point susceptibilities were also measured in molecular dynamics simulations [53,54] as well as in dense colloidal systems [52], all of which provide results that are qualitatively consistent with IMCT predictions. We also mention that the fifth-order susceptibilities recently measured in standard glass formers [80] are distinct from the ones derived in this work as ϑ_5 originate from variations of many-body correlators with respect to a conjugate field whereas the former are nonlinear susceptibilities originating from an expansion of the polarization tensor (whence the notation ϑ_{2n+1} , instead of χ_{2n+1}).

III. INSIGHTS FROM A ZERO-DIMENSIONAL LIMIT

A. Setting up the simplified model

It is clear that numerically solving for Eq. (8) is a Herculean task beyond $n = 1$ [78]. Indeed, Eq. (8) requires full solutions to oGMCT as initial conditions, which to this day have yet to be obtained [76]. In the spirit of early MCT [1–3] as well as early GMCT [81–83] studies, we therefore consider a schematic limit of the two coupled hierarchies Eqs. (5) and (8). The schematic approach amounts to restricting all physical processes to a single point in momentum space leading to an effective zero-dimensional, self-consistent relaxation

process, which captures the temporal behavior of the correlations of interest.

These models are obtained by setting the structure factor $S(k) = 1 + A\delta(k - k_0)$ where k_0 is the wave number of the first peak of the structure factor. Although simplified, schematic MCT and GMCT models are physically justified by the fact that the main peak of the static structure factor typically dominates over all other wave vectors [2,84]; additionally, the solutions of the schematic equations are known to share many qualitative features with the fully microscopic theory and, depending on the model parametrization, schematic and microscopic mode-coupling theories can be regarded as belonging to the same universality class [3].

In the overdamped limit, this schematic reduction yields the following two coupled hierarchies of integrodifferential equations:

$$\dot{\phi}_{2n}(t) + \mu_{2n}\phi_{2n} + \Lambda_{2n} \int_0^t d\tau M_{2n}^{(\phi)}(t - \tau)\dot{\phi}_{2n}(\tau) = 0, \quad (9)$$

where the memory kernel of a given correlator is defined as $M_{2n}^{(\phi)}(t) = \phi_{2(n+1)}(t)$ and is subject to initial conditions $\phi_{2n}(t = 0) = 1$. For the dynamical susceptibilities, we have

$$\begin{aligned} \dot{\vartheta}_{2n+1}(q; t) + \mu_{2n}\vartheta_{2n+1}(q; t) \\ + \Lambda_{2n} \int_0^t d\tau M_{2n}^{(\phi)}(t - \tau)\dot{\vartheta}_{2n+1}(q; t)(\tau) \\ + \tilde{\Lambda}_{2n}(q) \int_0^t d\tau M_{2n}^{(\vartheta)}(q; t - \tau)\dot{\phi}_{2n}(\tau) = \mathcal{T}_{2n}(t), \quad (10) \end{aligned}$$

subject to initial conditions $\vartheta_{2n+1}(q, t = 0) = 1$. This choice is justified by the fact that at zero time, the three-point susceptibility Eq. (3) is a product of three structure factors which are equal to unity in the simplified models considered here. To provide a link to the microscopic hierarchies the “mode-coupling” vertices \mathcal{V} are effectively mapped to a single coupling parameter Λ_{2n} , which can be interpreted as being proportional to an inverse temperature. In the case of MCT it can be shown that $\Lambda_2 = S(k_0)k_0A^2/8\pi^2\rho_0$ [2]. The bare frequencies Ω^2 and their variations with respect to the external field are mapped to real-valued parameters μ_{2n} and $\tilde{\mu}_{2n}$, respectively. Recall that the third term in Eq. (5) is simply a linear combination of the two-body bare frequency, hence for the models considered below we will set $\mu_{2n} = \tilde{\mu}_{2n} = n$, a wave-number-independent constant. Akin to Eq. (8), the simplified functional \mathcal{T}_{2n} contains the term with no susceptibilities and reads

$$\mathcal{T}_{2n} = -\tilde{\mu}_{2n}\phi_{2n}(t) - \Lambda_{2n} \int_0^t d\tau M_{2n}^{(\phi)}(t - \tau)\dot{\phi}_{2n}(\tau). \quad (11)$$

In the equations of motion for the dynamical susceptibility, a perturbative expansion of form $\tilde{\Lambda}_{2n}(q) \equiv \Lambda_{2n}(1 - \Gamma q^2)$ is used for the coupling constant, with $\Gamma \in \mathbb{R}$ such that $\Gamma q^2 < 1$. Following [46,85], this form is derived from symmetry considerations of the perturbative expansion of the critical mode-coupling eigenvalue. More simply, one expects an isotropic response in an isotropic medium, and thus only even powers of the perturbation wave vector are allowed. The generalization to higher-order correlation functions is reasonable because the many-body correlators exhibit the

same relaxation patterns as the two-body one since they are governed by equations of motion with similar mathematical form within the generalized mode-coupling theory [61]. We thus expect them to behave similarly near an eventual critical point. The wave-number dependence q associated with the infinitesimal perturbation is retained to study the behavior of the dynamical responses with respect to the “lengthscale” over which it is applied.

In the remainder of this work, we consider schematic IGMCT models with the same parametrizations as introduced in [81–83] for homogeneous GMCT. The three different parametrizations considered are as follows:

(1) Mayer-Miyazaki-Reichman (MMR):

$$\{\mu_{2n} = n; \Lambda_{2n} = \lambda\}; \quad (12)$$

(2) Linear Growth (LG):

$$\{\mu_{2n} = n; \Lambda_{2n} = \lambda(n + c)\}, \quad (13)$$

with $c \in \mathbb{R}$;

(3) Power Growth (PG)

$$\{\mu_{2n} = n; \Lambda_{2n} = \lambda n^{1-\nu}\}, \quad (14)$$

with $\nu \in \mathbb{R}$.

We note that in the base case where $n = 1$ and with a self-consistent closure of the form $M_2 \propto \phi_2(t)^2$, these models are all equivalent to the original Leutheusser model [1] up to a rescaling of the coupling constant. For simplicity, we will only consider the case where $\Gamma = 1$ in this work, as it only amounts to a rescaling of the wave-vector perturbation. The case of a negative Γ is not discussed here, but is mentioned in the case of the Leutheusser model in [46].

To obtain numerical results, we are forced to close the hierarchy at a given (arbitrary) height. The simplest closure is to set $\phi_{N_c}(t) = 0$, which is referred to as an exponential closure. This type of closure leads to avoided glass transitions as the correlators always decay to zero [82,83] and will be considered in a later work. The other common closure is referred to as a “mean-field” one, and consists in setting $\phi_{N_c}(t)$ equal to a monomial of lower-order correlators. More precisely, for the hierarchy height N_c at which self-consistency of the hierarchy is desired, we enforce that $M_{2N_c}^{(\phi)} = \prod_{j=1}^{N_c} \phi_{2i_j}(t)$, subject to the constraint $\sum_{j=1}^{N_c} i_j = N_c$. In this case, we systematically find that the system exhibits a glass transition at finite coupling strength [83]. Here, we formally define a glassy state as an ergodicity broken state; this corresponds to the set of points in parameter space beyond which the correlators $\phi_{2n}(t \rightarrow \infty) \equiv f_{2n} > 0$ no longer decay to zero. We denote the value of the plateaus of the correlators at the critical point by f_{2n}^c . Furthermore, we can numerically show that the correlators ϕ_{2n} display distinct asymptotic scaling behavior near the glass transition for a given mean-field closure [61,83]. In the early β -relaxation regime the correlators $\phi_{2n}(t)$ are governed by a power law decay $|f_{2n}^c - \phi_{2n}(t)| \propto t^{-a_n}$, while in the late β to early α regime one finds another power law behavior decay of the form $|f_{2n}^c - \phi_{2n}(t)| \propto t^{b_n}$. Additionally, the two relaxation times follow power laws, i.e., $\tau_\beta^{(2n)} \sim \epsilon^{-1/2a_n}$ and $\tau_\alpha^{(2n)} \sim \epsilon^{-\gamma_n}$ with $\gamma_n = 1/2a_n + 1/2b_n$. The exponents a_n, b_n are related by

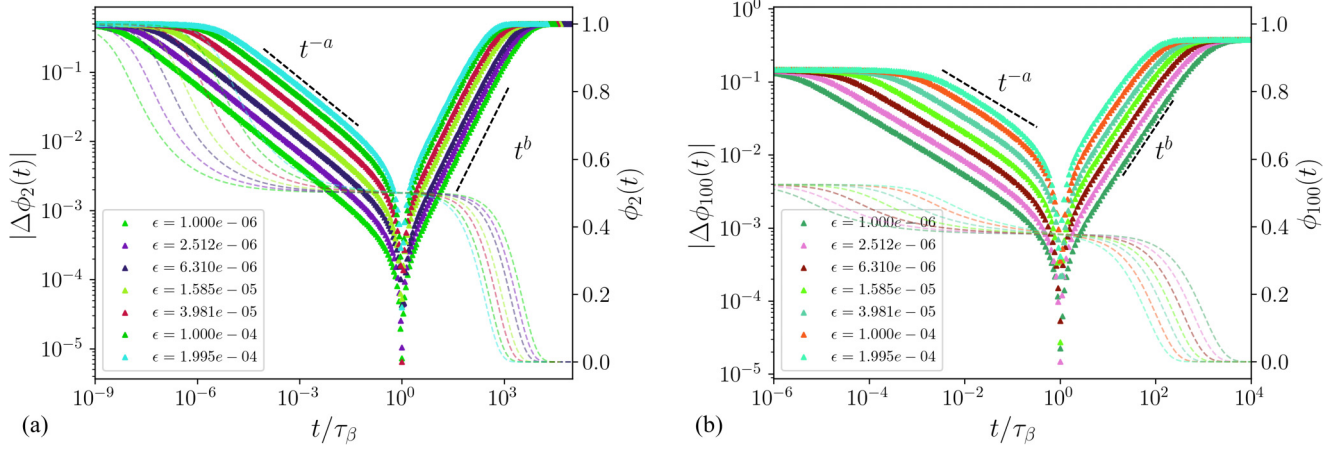


FIG. 1. (a) Full line: Relative trajectory of the correlator $\Delta\phi_2(t) \equiv \phi_2(t) - f_2^c$ on the left axis and full correlator $\phi_2(t)$ on the right axis for the Leutheusser model, at various distances ϵ from the critical point. The exponents are numerically determined to be $a = 0.395$ and $b = 1$, as expected from theory. Dashed line: Numerical solution for correlation $\phi_2(t)$. (b) Full line: Relative trajectory of the correlator $\Delta\phi_{100}(t) \equiv \phi_{100}(t) - f_{100}^c$ on the left axis and full correlator $\phi_{100}(t)$ on the right axis for the PG parametrization with $\nu = 0$ and self-consistent closure $M_{100}^{(\phi)}(t) = \phi_2(t)^{51}$, at various distances ϵ from the critical point. Dashed line: Numerical solution for correlation $\phi_{100}(t)$. The exponents are numerically determined to be $a = 0.395$ and $b = 1$, as expected from theory. Note that the time axis was rescaled by $\tau_\beta \equiv \epsilon^{-1/2a}$.

the well-known relation

$$\frac{\Gamma(1 - a_n)^2}{\Gamma(1 - 2a_n)} = \frac{\Gamma(1 + b_n)^2}{\Gamma(1 + 2b_n)}, \quad (15)$$

in the case where $N_c = 1$ [2,3], as displayed in Fig. 1(a) and for arbitrary mean-field closures of the MMR parametrization [83]. Furthermore, numerical results seem to confirm that the two other parametrizations (LG and PG) also obey this relation for mean-field closures. Hence as displayed in Fig. 1(b) for the PG parametrization with $\nu = 0$ and closure height $N_c = 100$, we numerically find that $a_{50} = 0.395$ and that $b_{50} = 1$. We report analogous findings for any level N_c , parametrizations and mean-field closure of the type previously defined.

The coupled hierarchies (9) and (10) are solved using an adaptation of the time doubling scheme presented in [86,87]. This type of numerical scheme has widely been used to solve mode-coupling-like integrodifferential equations.

B. Numerical results at finite order

We start in the liquid regime and approach the transition from the liquid side. Similarly to the simulation and experimental results [6,14,15], we find that our dynamical susceptibilities develop a sharp peak whose location coincides with that of the α -relaxation time τ_α of the corresponding correlation function, as shown in Figs. 2 and 3. Furthermore, for fixed coupling constant Λ_n , the additional correction levels from the GMCT hierarchy lead to a weakened response to external perturbations as the system is more liquid-like and effectively driven away from criticality by the increasing hierarchy height [81,83], as shown in Fig. 3 for the PG hierarchy. Similar behavior is observed for the other two parametrizations considered. This illustrates the principal success of the generalized mode-coupling theory: one obtains better quantitative predictions over a larger window of time and control

parameters, compared to the standard MCT which is known to overestimate the critical temperature.

The limit $q = 0$ corresponding to “macroscopic” perturbations’ lengthscales is considered first. In Fig. 2, results for the first three nonlinear susceptibilities $\vartheta_{3,5,7}(q = 0, t)$ with a PG parametrization, obtained from hierarchy heights $N_c = 1, 2, 3$, respectively, for varying distance to the critical point ϵ in the liquid regime are shown. There is a marked two-step power law growth $\vartheta_{2n+1}(q = 0, t) \propto t^{a_n}$ for $t < \tau_\beta^{(2n)}$ while $\vartheta_{2n+1}(q = 0, t) \propto t^{b_n}$ for $\tau_\beta^{(2n)} < t < \tau_\alpha^{(2n)}$ followed by a very fast decay of the dynamical susceptibilities for longer times. These results hold for susceptibilities of any order and the exponents a_n, b_n correspond to the well-known mode-coupling exponents previously mentioned and originally determined in [58]. Furthermore, we find that, at fixed distance to the critical point, this behavior is completely preserved.

We sketch a qualitative proof of the above observations. For simplicity we focus on the simpler MCT scenario with a single propagator and a single dynamical susceptibility. Then, $M^{(\phi)}(t) = \phi(t)^2$ and $M^{(\vartheta)}(q; t) = 2\phi(t)\vartheta(q; t)$. The argument extends to the GMCT scenario, but is less amenable to analytic treatment. Dropping all indices for further clarity, the density propagator in Laplace frequency space reads $\phi(z) = [z - \mu\Sigma(z)]^{-1}$ with $\Sigma(z) = [1 + \Lambda M^{(\phi)}(z)]^{-1}$ some (nonperturbative) correction. Similarly the linear equation for the dynamical susceptibility can be written as $\vartheta(q; z)[z + f(q; z)] = T(z)$ where

$$f(q; z) = \mu + 2\tilde{\Lambda}(q)\phi(z)(z\phi(z) - 1) + z\Lambda M^{(\phi)}(z), \quad (16)$$

and $T(z)$ some regular function of z . It follows that $\vartheta(q; z)$ grows as $[z + f(q; z)]$ decreases and eventually diverges once $[z + f(q; z)] = 0$. Under the assumption that $M^{(\phi)}(z) \propto 1/z$ (which we self-consistently check later), it is easy to show that the condition $[z + f(q; z)] = 0$ is a quadratic equation in $\phi(z)$ whose solution admits the following form $\phi(z) \propto 1/z + \mathcal{O}(z)$ in the limit $z \ll 1$. Translating back to the time domain, we

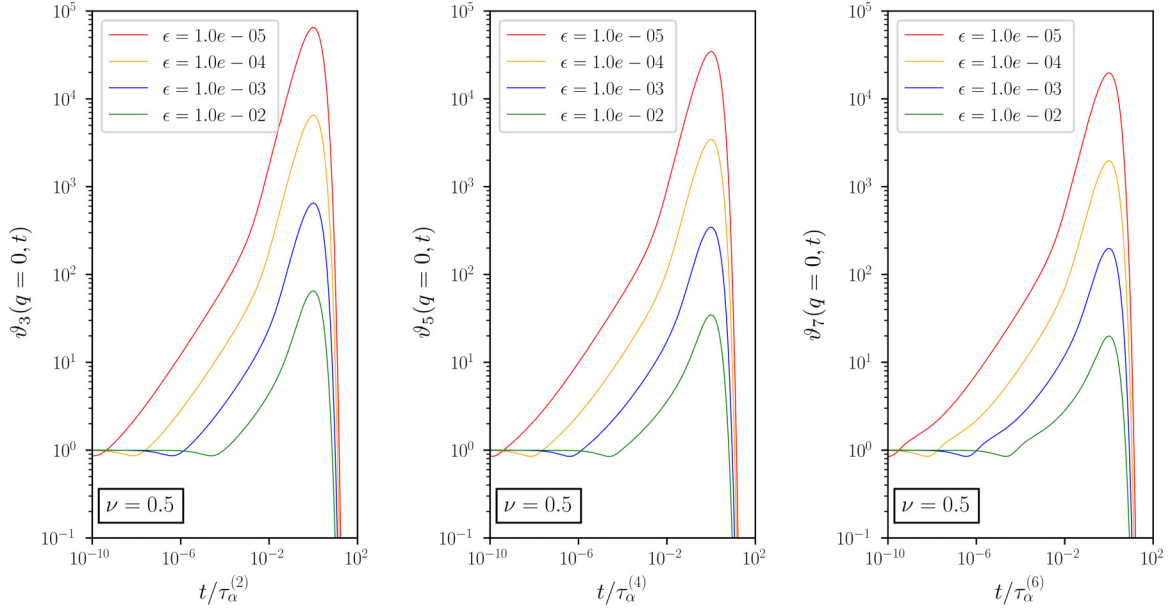


FIG. 2. Multipoint dynamical susceptibilities ϑ_3 , ϑ_5 , ϑ_7 at different distances ϵ to the critical point from the liquid regime for the PG parametrization with parameter $\nu = 0.5$ and closures $M_2^{(\phi)}(t) = \phi_2(t)^2$, $M_4^{(\phi)}(t) = \phi_2(t)^4$, $M_6^{(\phi)}(t) = \phi_2(t)^6$ for hierarchy heights $N_c = 1, 2, 3$ in left, center, and right panels, respectively. The time axis is rescaled with respect to α -relaxation times $\tau_\alpha^{(2n)}$ as defined in the main text.

have that the dynamical susceptibility $\vartheta(t)$ will grow whenever $\phi(t)$ and $M^{(\phi)}(t)$ (by assumption) are slowly varying over macroscopic timescales. This is precisely what happens at the onset of glass-like behavior where propagators exhibit double step decays with an intermediate plateau, as displayed in the upper panel of Fig. 3. This calculation also demonstrates how the dynamical susceptibilities inherit the scaling exponents of the propagators, but with a reversed sign due to the operator

inversion. We anticipate that this argument also extends to the fully microscopic theory since the mathematical structure of the time dependence is unchanged.

Moreover, we find that the peak of the dynamical susceptibilities scales in a similar way to what is found in [34]. Indeed, the maximum of the dynamical response of any order scales as a power law $\vartheta_{2n+1}^*(q=0) \propto \epsilon^\Delta$ with exponent $\Delta = -1$ as the transition is approached, irrespective of the global hierarchy level and of the parametrization of the coupling coefficients Λ_{2n} , as displayed in Fig. 4 for the PG and MMR parametrizations. We find the same results for the LG parametrization, though not shown in the main text. This illustrates the robustness of the scaling laws of the initial theory as N_c is increased.

The above observations imply that the scaling laws governing the divergence of the nonlinear dynamical susceptibilities are universal near the simplest glass transition, regardless of the chosen parametrizations. This universality is expected to hold for all systems exhibiting \mathcal{A}_2 -glass singularities, as the equations of motion can be appropriately mapped to their normal form close enough to the transition point [3]. Akin to the correlators, the dynamical susceptibilities are found to converge with increasing hierarchy height at fixed coupling. This is in line with prior results on schematic GMCT, which show a manifestly convergent behavior as the hierarchy height is increased while keeping the coupling strength fixed [81,82]. Moreover, numerical results in the case of the homogeneous microscopic theory substantiate this [57,59–61]. We therefore expect that the solutions to the microscopic equations in Eq. (8) eventually converge with increasing hierarchy height at fixed points in parameter space. However, convergence is not necessarily expected at fixed relative distance to the critical point for increasing hierarchy height. We now turn towards the study of both the q and time-dependent scaling of dynamical susceptibilities. Figure 5 reports on the magnitude of the dynamical responses at different timescales as a function of

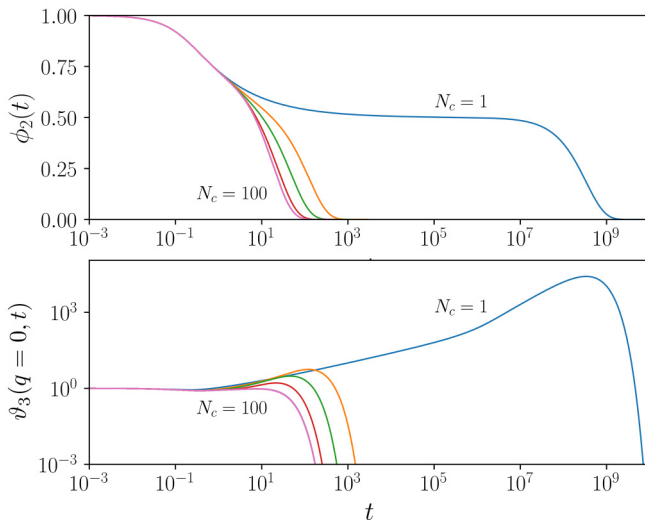


FIG. 3. Top panel: Principal correlator $\phi_2(t)$ at fixed coupling constant $\Lambda_2 = 4 - \delta$ with $\delta = 10^{-4}$. We use the PG parametrization with $\nu = 1$ and display the correlation function $\phi_2(t)$ for increasing hierarchy height $N_c = 1, 2, 5, 10, 100$ appearing in increasing order from uppermost to lowermost curves. Bottom panel: Three-point dynamical susceptibility associated with the correlator of the top panel.

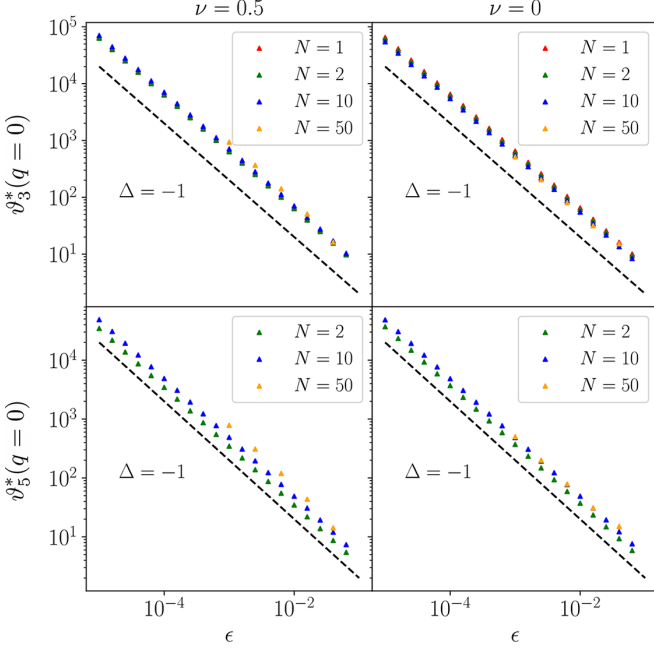


FIG. 4. Power law scaling behavior of the maximum of the first two susceptibilities $\vartheta_3^*(q=0)$, $\vartheta_5^*(q=0)$ in the PG hierarchy with $\nu = 1/2, 0$, as a function of the distance ϵ to the glass transition with various hierarchy heights. Note that at $\nu = 0$, the PG parametrization is equivalent to the MMR one.

the perturbation ‘lengthscale’ q^{-1} . As previously noted, the response grows in time, reaching its peak at the α -relaxation time, which suggests the existence of a saturated dynamical lengthscale. Furthermore, the magnitude of the response is strongly q dependent at all time scales. Indeed, the dynamical responses reach a maximum for some threshold macroscopic perturbation lengthscale q_* , indicating that these are genuine collective responses. From Fig. 5, we see that q_* depends on both the timescales probed as well as the distance to the glass transition. Overall, denoting ξ_{2n} the lengthscale associated with the $2n + 1$ th dynamical susceptibility, a global scaling of the form

$$\vartheta_{2n+1}(q, t) \approx (\xi_{2n})^2 g_{2n+1}(\xi_{2n} q, t/\tau_\beta^{(2n)}) \quad (17)$$

is observed for the nonlinear susceptibilities at all orders n . This is a generalization of the scaling for the higher-order susceptibilities initially determined in [46,88]. This generalization is justified since we know that the correlators within GMCT retain the same critical properties as those of MCT, as illustrated in Fig. 1. It thus naturally follows that the susceptibilities should as well. We therefore generalize [46] and write

$$g_{2n+1}(x, y) = \frac{1}{\alpha_n y^{-a_n} + x^2} + \frac{\beta_n y^{b_n}}{1 + x^2 + \gamma_n y^{c_n} x^4},$$

where $\alpha_n, \beta_n, \gamma_n$ are real-valued coefficients which depend on the choice of parametrization of the hierarchies Eqs. (9) and (10). The prefactor ξ_{2n}^2 in Eq. (17) is a consequence of the Lorentzian form of the first term of the scaling function. The exponents a_n, b_n are the GMCT exponents previously introduced and c_n governs the growth of the quartic tail seen

in Fig. 5 beyond the β -relaxation regime, where the scaling law breaks down. We numerically determine that c_n lies in the range (0.15, 0.20) for the three parametrizations considered, in line with earlier results [46]. We also comment on the range of validity of the scaling law, which is numerically determined to hold in the early β regime [up to $t/\tau_\beta \sim \mathcal{O}(10^{-5})$] but starts to fail in the late β regime [beyond $t/\tau_\beta \sim \mathcal{O}(10^2)$], as displayed in Fig. 5(a) for the MMR parametrization, where we see the growth of a quartic tail, responsible for the α scaling, which was previously discussed in [46]. We observe the same behavior for the fifth-order susceptibility as shown in Fig. 5(b), which suggests that the postulated generalization is valid. Similar findings are reported for higher-order susceptibilities and also the different parametrizations considered. In the limit $x \rightarrow 0$ the sequential power-law behavior $\vartheta_{2n+1}(q=0, t) = \alpha_n^{-1} (t/\tau_\beta^{(2n)})^{a_n} + \beta_n (t/\tau_\beta^{(2n)})^{b_n}$ observed in the numerical solutions shown in Fig. 2 and detailed in the text is recovered. In the $\alpha^{(2n)}$ -relaxation regime (i.e., $t/\tau_\beta^{(2n)} \gg 1$) and at low wave numbers ($q \rightarrow 0$) we find since $a_n = 0.395$ and $b_n = 1$ that the peak of the susceptibility must scale according to

$$\vartheta_{2n+1}^*(q) \approx \xi_{2n}^2 \beta_n (\tau_\alpha^{(2n)}/\tau_\beta^{(2n)})^{b_n} \propto \epsilon^{-\Delta},$$

as numerically determined. Using $(\tau_\alpha^{(2n)}/\tau_\beta^{(2n)})^{b_n} = \epsilon^{-1/2}$ [82], we conclude that there exists a set of diverging lengthscales going as $\xi_{2n} \propto \epsilon^{-1/4}$ at the α -relaxation timescale (since $\Delta = -1$). Thus, a set of true diverging dynamical lengthscales associated with dynamical susceptibilities of any order is expected at the ideal glass transition, where the separation parameter ϵ vanishes.

IV. COMMENT ON INFINITE HIERARCHIES

Finally, it is interesting to briefly consider the limit $n \rightarrow \infty$ of Eqs. (9) and (10). We recall that for the MMR model, previous studies demonstrated that this particular limit washed away any critical singularity and that the α -relaxation timescale did not diverge at the finite-coupling constant for particular parametrizations of the bare frequencies and coupling constants, we instead find that $\tau_\alpha^{(2)} \propto \lambda^{-1} e^\lambda$ [81,83]. This implies that the dynamical susceptibilities introduced here no longer critically diverge at the finite-coupling constant as the limit of infinite hierarchy height is taken. Nonetheless, numerical treatment of the infinite hierarchy (9) showed that it exhibits the very same MCT power law scalings a_n, b_n , and γ_n in a limited parameter range $3 \leq \lambda \leq 9$ [81]. Hence, a quantitative agreement between finite and infinite hierarchies within the same coupling constant window is expected and we therefore anticipate the susceptibilities to grow with the same exponents as at finite order. In the case of the LG parametrization, we know that it admits a discontinuous transition at $\lambda_c = 1$, with a divergence of the relaxation time going as a power law $\tau_\alpha^{(2)} \propto (\lambda_c - \lambda_2)^{-c}$ [83]. This scenario is very similar to that of the mean-field closures considered in the previous section, albeit with a different exponent for the divergence of the relaxation time. Lastly, the PG parametrization with a non-self-consistent closure has shown in the past to display avoided transitions at finite Λ_2 [82]. Interestingly, tuning the parameter ν enables the hierarchy to display different fragility

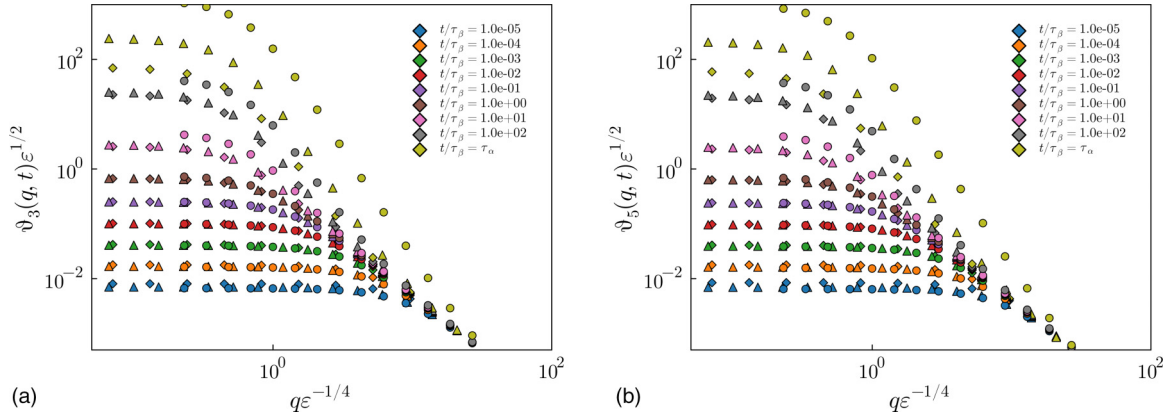


FIG. 5. (a) Verification of the scaling relation Eq. (4) for the third-order nonlinear susceptibility of the MMR model with $N_c = 1$ at distances $\epsilon = 10^{-7}, 10^{-6}, 10^{-5}$ from the critical point, which are shown with circle, triangle, and diamond markers, respectively. (b) Verification of the scaling relation (4) for the fifth-order nonlinear susceptibility of the MMR model with $N_c = 2$ at distances $\epsilon = 10^{-7}, 10^{-6}, 10^{-5}$ from the critical point, which are shown with circle, triangle, and diamond markers, respectively.

behavior, a feature which is not accessible to the standard MCT. It would therefore be of interest to study the behavior of the simplified dynamic susceptibilities with respect to the kinetic fragility index.

V. CONCLUSION

In this work the GMCT of the glass transition is extended to the presence of an external pinning field that locally modulates the microscopic density. By treating the resulting equations of motion as a Landau theory and making use of the fact that GMCT incorporates an arbitrary number of many-body dynamic structure factors, a set of self-consistent equations of motion for previously unstudied nonlinear dynamical susceptibilities ϑ_{2n+1} is found. The equations of motion for nonlinear dynamical susceptibilities can be casted into an eigenvalue problem and it is hypothesised that a true diverging susceptibility, and hence a diverging dynamic lengthscale exists at the (generalized) mode-coupling critical point. This hypothesis is corroborated by earlier results on the fully microscopic mode-coupling theory [45,46,78] and on analogous simpler self-consistent relaxation models which are shown to capture the phenomenology of the wave-vector-dependent MCT equations [1,3,58,81]. Near the simplest glass singularity predicted by mode-coupling theories, diverging susceptibilities of any order asymptotically close to the critical point are found. Akin to [46,79], the dynamic lengthscales ξ_{2n}^* of any order are found to saturate at the α -relaxation time and are numerically found to diverge as $\epsilon^{-1/4}$ as the critical point is approached. The value of this exponent is in line with microscopic calculations of MCT [79] but does not coincide with results from molecular dynamics simulations [41,54], which find that the dynamic lengthscale diverges as $\epsilon^{-1/2}$ in both hard and soft sphere

systems. Recent results for fragile liquids, however, seem to be in line with an MCT-like scenario, where a dynamical lengthscale diverging as $\epsilon^{-0.3}$ was reported [89]. The scaling behavior of the susceptibilities was studied in both space and time and in various limits of the physical parameters for the simplified self-consistent relaxation models. Nonetheless, the analysis of the simplified self-consistent models further strengthens the idea that the MCT scenario is an incredibly robust one.

The nonlinear dynamical susceptibilities introduced in this work provide us with new tools to make quantitative predictions on this still poorly understood facet of glass physics. We reserve a detailed analytic and numerical study of the scaling laws near the set of higher-order glass singularities predicted by the microscopic generalized mode-coupling theory [90,91], extending on [85], for future work. Furthermore, it would be interesting to measure these nonlinear susceptibilities in molecular glass formers, inhomogeneous MD simulations, or in simpler model glass forming systems such as kinetically constrained models as was recently suggested in [92].

ACKNOWLEDGMENTS

We thank G. Biroli for showing us the explicit form of the scaling function for the three-point susceptibility, which allowed us to generalize the result. We thank I. Pihlajamaa for useful comments on the manuscript as well as for numerous discussions on the numerical routines. The authors acknowledge financial support from the Dutch Research Council (NWO) through a Vidi grant (C.C.L.L. and L.M.C.J.) and START-UP grant (C.L. and L.M.C.J.).

- [1] E. Leutheusser, Dynamical model of the liquid-glass transition, *Phys. Rev. A* **29**, 2765 (1984).
- [2] U. Bengtzelius, W. Gotze, and A. Sjolander, Dynamics of supercooled liquids and the glass transition, *J. Phys. C: Solid State Phys.* **17**, 5915 (1984).

- [3] W. Götze, *Complex Dynamics of Glass-Forming Liquids: A Mode-Coupling Theory*, Vol. 143, (Oxford University Press, Oxford, 2008).
- [4] G. Parisi and F. Zamponi, Mean-field theory of hard sphere glasses and jamming, *Rev. Mod. Phys.* **82**, 789 (2010).

- [5] M. Mezard and G. Parisi, Glasses and replicas, in *Structural Glasses and Supercooled Liquids: Theory, Experiment, and Applications* (Wiley, New York, 2012), p. 151.
- [6] W. Kob, C. Donati, S. J. Plimpton, P. H. Poole, and S. C. Glotzer, Dynamical Heterogeneities in a Supercooled Lennard-Jones Liquid, *Phys. Rev. Lett.* **79**, 2827 (1997).
- [7] C. Donati, J. F. Douglas, W. Kob, S. J. Plimpton, P. H. Poole, and S. C. Glotzer, Stringlike Cooperative Motion in a Supercooled Liquid, *Phys. Rev. Lett.* **80**, 2338 (1998).
- [8] A. H. Marcus, J. Schofield, and S. A. Rice, Experimental observations of Non-Gaussian behavior and stringlike cooperative dynamics in concentrated quasi-two-dimensional colloidal liquids, *Phys. Rev. E* **60**, 5725 (1999).
- [9] W. K. Kegel and A. van Blaaderen, Direct observation of dynamical heterogeneities in colloidal hard-sphere suspensions, *Science* **287**, 290 (2000).
- [10] E. V. Russell and N. Israeloff, Direct observation of molecular cooperativity near the glass transition, *Nature (London)* **408**, 695 (2000).
- [11] S. C. Glotzer, Spatially heterogeneous dynamics in liquids: Insights from simulation, *J. Non-Cryst. Solids* **274**, 342 (2000).
- [12] B. Doliwa and A. Heuer, Cooperativity and spatial correlations near the glass transition: Computer simulation results for hard spheres and disks, *Phys. Rev. E* **61**, 6898 (2000).
- [13] E. R. Weeks, J. C. Crocker, A. C. Levitt, A. Schofield, and D. A. Weitz, Three-dimensional direct imaging of structural relaxation near the colloidal glass transition, *Science* **287**, 627 (2000).
- [14] N. Lačević, F. W. Starr, T. Schröder, and S. Glotzer, Spatially heterogeneous dynamics investigated via a time-dependent four-point density correlation function, *J. Chem. Phys.* **119**, 7372 (2003).
- [15] L. Berthier, G. Biroli, J.-P. Bouchaud, L. Cipelletti, and W. van Saarloos, *Dynamical Heterogeneities in Glasses, Colloids, and Granular Media*, Vol. 150 (Oxford University Press, Oxford, 2011).
- [16] Z. Zhang, P. J. Yunker, P. Habdas, and A. G. Yodh, Cooperative Rearrangement Regions and Dynamical Heterogeneities in Colloidal Glasses with Attractive Versus Repulsive Interactions, *Phys. Rev. Lett.* **107**, 208303 (2011).
- [17] K. Kim and S. Saito, Multiple length and time scales of dynamic heterogeneities in model glass-forming liquids: A systematic analysis of multi-point and multi-time correlations, *J. Chem. Phys.* **138**, 12A506 (2013).
- [18] A. Wisitsorasak and P. G. Wolynes, Dynamical heterogeneity of the glassy state, *J. Phys. Chem. B* **118**, 7835 (2014).
- [19] I. Tah, A. Mutneja, and S. Karmakar, Understanding slow and heterogeneous dynamics in model supercooled glass-forming liquids, *ACS Omega* **6**, 7229 (2021).
- [20] G. Adam and J. H. Gibbs, On the temperature dependence of cooperative relaxation properties in glass-forming liquids, *J. Chem. Phys.* **43**, 139 (1965).
- [21] O. Dauchot, G. Marty, and G. Biroli, Dynamical Heterogeneity Close to the Jamming Transition in a Sheared Granular Material, *Phys. Rev. Lett.* **95**, 265701 (2005).
- [22] K. E. Avila, H. E. Castillo, A. Fiege, K. Vollmayr-Lee, and A. Zippelius, Strong Dynamical Heterogeneity and Universal Scaling in Driven Granular Fluids, *Phys. Rev. Lett.* **113**, 025701 (2014).
- [23] J.-A. Park, J. H. Kim, D. Bi, J. A. Mitchel, N. T. Qazvini, K. Tantisira, C. Y. Park, M. McGill, S.-H. Kim, B. Gweon *et al.*, Unjamming and cell shape in the asthmatic airway epithelium, *Nat. Mater.* **14**, 1040 (2015).
- [24] C. Malinverno, S. Corallino, F. Giavazzi, M. Bergert, Q. Li, M. Leoni, A. Disanza, E. Frittoli, A. Oldani, E. Martini *et al.*, Endocytic reawakening of motility in jammed epithelia, *Nat. Mater.* **16**, 587 (2017).
- [25] L. M. Janssen, Active glasses, *J. Phys.: Condens. Matter* **31**, 503002 (2019).
- [26] G. Janzen and L. M. C. Janssen, Aging in thermal active glasses, *Phys. Rev. Res.* **4**, L012038 (2022).
- [27] E. Boattini, S. Marín-Aguilar, S. Mitra, G. Foffi, F. Smallegang, and L. Filion, Autonomously revealing hidden local structures in supercooled liquids, *Nat. Commun.* **11**, 5479 (2020).
- [28] G. A. Appignanesi, J. A. Rodriguez Fris, R. A. Montani, and W. Kob, Democratic Particle Motion for Metabasin Transitions in Simple Glass Formers, *Phys. Rev. Lett.* **96**, 057801 (2006).
- [29] F. W. Starr, J. F. Douglas, and S. Sastry, The relationship of dynamical heterogeneity to the Adam-Gibbs and random first-order transition theories of glass formation, *J. Chem. Phys.* **138**, 12A541 (2013).
- [30] A. Smessaert and J. Rottler, Distribution of local relaxation events in an aging three-dimensional glass: Spatiotemporal correlation and dynamical heterogeneity, *Phys. Rev. E* **88**, 022314 (2013).
- [31] L. Berthier, Dynamic heterogeneity in Amorphous materials, *Physics* **4**, 42 (2011).
- [32] N. Lacević and S. Glotzer, Approach to the glass transition studied by higher order correlation functions, *J. Phys.: Condens. Matter* **15**, S2437 (2003).
- [33] M. Vogel and S. C. Glotzer, Temperature dependence of spatially heterogeneous dynamics in a model of viscous silica, *Phys. Rev. E* **70**, 061504 (2004).
- [34] C. Dalle-Ferrier, C. Thibierge, C. Alba-Simionesco, L. Berthier, G. Biroli, J.-P. Bouchaud, F. Ladieu, D. L'Hôte, and G. Tarjus, Spatial correlations in the dynamics of glassforming liquids: Experimental determination of their temperature dependence, *Phys. Rev. E* **76**, 041510 (2007).
- [35] E. Flenner and G. Szamel, Anisotropic spatially heterogeneous dynamics on the α and β relaxation time scales studied via a four-point correlation function, *Phys. Rev. E* **79**, 051502 (2009).
- [36] L. Berthier, G. Biroli, J.-P. Bouchaud, W. Kob, K. Miyazaki, and D. Reichman, Spontaneous and induced dynamic fluctuations in glass formers. i. general results and dependence on ensemble and dynamics, *J. Chem. Phys.* **126**, 184503 (2007).
- [37] L. Berthier, G. Biroli, J.-P. Bouchaud, W. Kob, K. Miyazaki, and D. R. Reichman, Spontaneous and induced dynamic correlations in glass formers. ii. model calculations and comparison to numerical simulations, *J. Chem. Phys.* **126**, 184504 (2007).
- [38] E. R. Weeks and D. A. Weitz, Properties of Cage Rearrangements Observed near the Colloidal Glass Transition, *Phys. Rev. Lett.* **89**, 095704 (2002).
- [39] A. S. Keys, A. R. Abate, S. C. Glotzer, and D. J. Durian, Measurement of growing dynamical length scales and prediction of the jamming transition in a granular material, *Nat. Phys.* **3**, 260 (2007).
- [40] E. R. Weeks, J. C. Crocker, and D. A. Weitz, Short- and long-range correlated motion observed in colloidal

- glasses and liquids, *J. Phys.: Condens. Matter* **19**, 205131 (2007).
- [41] E. Flenner, M. Zhang, and G. Szamel, Analysis of a growing dynamic length scale in a glass-forming binary hard-sphere mixture, *Phys. Rev. E* **83**, 051501 (2011).
- [42] E. Flenner, H. Staley, and G. Szamel, Universal Features of Dynamic Heterogeneity in Supercooled Liquids, *Phys. Rev. Lett.* **112**, 097801 (2014).
- [43] A. Andreanov, G. Biroli, and J.-P. Bouchaud, Mode coupling as a Landau theory of the glass transition, *Europhys. Lett.* **88**, 16001 (2009).
- [44] G. Biroli and J.-P. Bouchaud, Diverging length scale and upper critical dimension in the mode-coupling theory of the glass transition, *Europhys. Lett.* **67**, 21 (2004).
- [45] J.-P. Bouchaud and G. Biroli, Nonlinear susceptibility in glassy systems: A probe for cooperative dynamical length scales, *Phys. Rev. B* **72**, 064204 (2005).
- [46] G. Biroli, J.-P. Bouchaud, K. Miyazaki, and D. R. Reichman, Inhomogeneous Mode-Coupling Theory and Growing Dynamic Length in Supercooled Liquids, *Phys. Rev. Lett.* **97**, 195701 (2006).
- [47] L. Berthier, G. Biroli, J.-P. Bouchaud, L. Cipelletti, D. El Masri, D. L'Hôte, F. Ladieu, and M. Pierno, Direct experimental evidence of a growing length scale accompanying the glass transition, *Science* **310**, 1797 (2005).
- [48] C. Crauste-Thibierge, C. Brun, F. Ladieu, D. L'hôte, G. Biroli, and J.-P. Bouchaud, Evidence of Growing Spatial Correlations at the Glass Transition from Nonlinear Response Experiments, *Phys. Rev. Lett.* **104**, 165703 (2010).
- [49] C. Brun, F. Ladieu, D. L'Hôte, M. Tarzia, G. Biroli, and J.-P. Bouchaud, Nonlinear dielectric susceptibilities: Accurate determination of the growing correlation volume in a supercooled liquid, *Phys. Rev. B* **84**, 104204 (2011).
- [50] T. Bauer, P. Lunkenheimer, and A. Loidl, Cooperativity and the Freezing of Molecular Motion at the Glass Transition, *Phys. Rev. Lett.* **111**, 225702 (2013).
- [51] R. Casalini, D. Fragiadakis, and C. Roland, Dynamic correlation length scales under isochronal conditions, *J. Chem. Phys.* **142**, 064504 (2015).
- [52] C. K. Mishra, P. Haddas, and A. Yodh, Dynamic heterogeneities in colloidal supercooled liquids: Experimental tests of inhomogeneous mode coupling theory, *J. Phys. Chem. B* **123**, 5181 (2019).
- [53] G. Brambilla, D. El Masri, M. Pierno, L. Berthier, L. Cipelletti, G. Petekidis, and A. B. Schofield, Probing the Equilibrium Dynamics of Colloidal Hard Spheres above the Mode-Coupling Glass Transition, *Phys. Rev. Lett.* **102**, 085703 (2009).
- [54] K. Kim, S. Saito, K. Miyazaki, G. Biroli, and D. R. Reichman, Dynamic length scales in glass-forming liquids: An inhomogeneous molecular dynamics simulation approach, *J. Phys. Chem. B* **117**, 13259 (2013).
- [55] D. R. Reichman and P. Charbonneau, Mode-coupling theory, *J. Stat. Mech.: Theory Exp.* (2005) P05013.
- [56] L. M. Janssen, Mode-coupling theory of the glass transition: A primer, *Front. Phys.* **6**, 97 (2018).
- [57] G. Szamel, Colloidal Glass Transition: Beyond Mode-Coupling Theory, *Phys. Rev. Lett.* **90**, 228301 (2003).
- [58] L. M. C. Janssen and D. R. Reichman, Microscopic Dynamics of Supercooled Liquids from First Principles, *Phys. Rev. Lett.* **115**, 205701 (2015).
- [59] J. Wu and J. Cao, High-Order Mode-Coupling Theory for the Colloidal Glass Transition, *Phys. Rev. Lett.* **95**, 078301 (2005).
- [60] C. Luo and L. M. C. Janssen, Generalized mode-coupling theory of the glass transition. ii. analytical scaling laws, *J. Chem. Phys.* **153**, 214506 (2020).
- [61] C. Luo and L. M. C. Janssen, Generalized mode-coupling theory of the glass transition. i. numerical results for Percus–Yevick hard spheres, *J. Chem. Phys.* **153**, 214507 (2020).
- [62] V. E. Debets, C. Luo, S. Ciarella, and L. M. C. Janssen, Generalized mode-coupling theory for mixtures of brownian particles, *Phys. Rev. E* **104**, 065302 (2021).
- [63] S. Ciarella, C. Luo, V. E. Debets, and L. Janssen, Multi-component generalized mode-coupling theory: Predicting dynamics from structure in glassy mixtures, *Eur. Phys. J. E* **44**, 91 (2021).
- [64] C. Luo, V. E. Debets, and L. M. Janssen, Tagged-particle motion of Percus–Yevick hard spheres from first principles, *J. Chem. Phys.* **155**, 034502 (2021).
- [65] H. Mori, Transport, collective motion, and Brownian motion, *Prog. Theor. Phys.* **33**, 423 (1965).
- [66] H. Mori, A continued-fraction representation of the time-correlation functions, *Prog. Theor. Phys.* **34**, 399 (1965).
- [67] R. Zwanzig, *Nonequilibrium Statistical Mechanics* (Oxford University Press, Oxford, 2001).
- [68] J.-P. Hansen and I. R. McDonald, *Theory of Simple Liquids: With Applications to Soft Matter* (Academic, New York, 2013).
- [69] See Supplemental Material at <http://link.aps.org/supplemental/10.1103/PhysRevE.106.064136> for more information and additional resources.
- [70] J. Schofield, R. Lim, and I. Oppenheim, Mode coupling and generalized hydrodynamics, *Physica A* **181**, 89 (1992).
- [71] M. Manno and I. Oppenheim, Microscopic theory for hopping transport in glass-forming liquids: Mode coupling corrections, *Physica A* **265**, 520 (1999).
- [72] G. Szamel, Dynamics of interacting brownian particles: A diagrammatic formulation, *J. Chem. Phys.* **127**, 084515 (2007).
- [73] G. Szamel, Mode-coupling theory and beyond: A diagrammatic approach, *Prog. Theor. Exp. Phys.* **2013**, 012J01 (2013).
- [74] J. Barrat, J. Hansen, and G. Pastore, On the equilibrium structure of dense fluids: Triplet correlations, integral equations and freezing, *Mol. Phys.* **63**, 747 (1988).
- [75] J. Bosse, W. Götze, and M. Lücke, Mode-coupling theory of simple classical liquids, *Phys. Rev. A* **17**, 434 (1978).
- [76] S. Ciarella, Relaxation Pathways for Soft Materials, Ph.D. thesis, Technische Universiteit Eindhoven Eindhoven, 2021.
- [77] K. Miyazaki, Nonlinear susceptibility of glassy systems, (unpublished).
- [78] G. Szamel and E. Flenner, Three-point susceptibilities $\chi_n(k; t)$ and $\chi_n^s(k; t)$: Mode-coupling approximation, *Phys. Rev. E* **79**, 021503 (2009).
- [79] G. Szamel and E. Flenner, Diverging length scale of the inhomogeneous mode-coupling theory: A numerical investigation, *Phys. Rev. E* **81**, 031507 (2010).
- [80] S. Albert, T. Bauer, M. Michl, G. Biroli, J.-P. Bouchaud, A. Loidl, P. Lunkenheimer, R. Tourbot, C. Wiertel-Gasquet, and F. Ladieu, Fifth-order susceptibility unveils growth of thermodynamic amorphous order in glass-formers, *Science* **352**, 1308 (2016).

- [81] P. Mayer, K. Miyazaki, and D. R. Reichman, Cooperativity beyond Caging: Generalized Mode-Coupling Theory, *Phys. Rev. Lett.* **97**, 095702 (2006).
- [82] L. M. C. Janssen, P. Mayer, and D. R. Reichman, Relaxation patterns in supercooled liquids from generalized mode-coupling theory, *Phys. Rev. E* **90**, 052306 (2014).
- [83] L. M. C. Janssen, P. Mayer, and D. R. Reichman, Generalized mode-coupling theory of the glass transition: Schematic results at finite and infinite order, *J. Stat. Mech. Theory Exp.* (2016) 054049.
- [84] S. Ciarella, R. A. Biezemans, and L. M. Janssen, Understanding, predicting, and tuning the fragility of vitrimeric polymers, *Proc. Natl. Acad. Sci. USA* **116**, 25013 (2019).
- [85] S. K. Nandi, G. Biroli, J.-P. Bouchaud, K. Miyazaki, and D. R. Reichman, Critical Dynamical Heterogeneities Close to Continuous Second-Order Glass Transitions, *Phys. Rev. Lett.* **113**, 245701 (2014).
- [86] M. Fuchs, W. Gotze, I. Hofacker, and A. Latz, Comments on the alpha-peak shapes for relaxation in supercooled liquids, *J. Phys.: Condens. Matter* **3**, 5047 (1991).
- [87] E. Flenner and G. Szamel, Relaxation in a glassy binary mixture: Comparison of the mode-coupling theory to a brownian dynamics simulation, *Phys. Rev. E* **72**, 031508 (2005).
- [88] M. Tarzia, G. Biroli, A. Lefèvre, and J.-P. Bouchaud, Anomalous nonlinear response of glassy liquids: General arguments and a mode-coupling approach, *J. Chem. Phys.* **132**, 054501 (2010).
- [89] I. Tah and S. Karmakar, Kinetic fragility directly correlates with the many-body static amorphous order in glass-forming liquids, *Phys. Rev. Mater.* **6**, 035601 (2022).
- [90] W. Götze and M. Sperl, Logarithmic relaxation in glass-forming systems, *Phys. Rev. E* **66**, 011405 (2002).
- [91] C. Luo and L. M. C. Janssen, Glassy dynamics of sticky hard spheres beyond the mode-coupling regime, *Soft Matter* **17**, 7645 (2021).
- [92] G. Biroli, J.-P. Bouchaud, and F. Ladieu, Amorphous order and nonlinear susceptibilities in glassy materials, *J. Phys. Chem. B* **125**, 7578 (2021).